

- <sup>19</sup>E. G. Wilson and S. A. Rice, Phys. Rev. 145, 55 (1966).  
<sup>20</sup>T. E. Faber, Advan. Phys. 15, 547 (1966).  
<sup>21</sup>J. S. Helman and W. Baltensperger, Phys. Kondens. Materie 5, 60 (1966).  
<sup>22</sup>R. L. Schroeder and J. C. Thompson, Phys. Rev. 179, 124 (1969).  
<sup>23</sup>W. L. Jolly and C. Hallada, Inorg. Chem. 2, 1076 (1963).  
<sup>24</sup>M. N. Alexander and D. F. Holcomb, Rev. Mod. Phys. 40, 815 (1968).

PHYSICAL REVIEW A

VOLUME 1, NUMBER 2

FEBRUARY 1970

## Dynamic Coupling Phenomena in Molecular Excited States. I. General Formulation and Vibronic Coupling H<sub>2</sub>

R. Stephen Berry

*Department of Chemistry and The James Franck Institute, University of Chicago, Chicago, Illinois 60637*

and

Svend Erik Nielsen

*Chemistry Laboratory III, H. C. Ørsted Institute, University of Copenhagen, Copenhagen 2100, Denmark*

(Received 4 August 1969)

A general formalism is described for treating diabatic coupling processes in highly excited molecular states. The method treats electronic and nuclear motion quantum mechanically, and uses the adiabatic Born-Oppenheimer states as basis functions. The present paper concentrates on diagnoses of vibronic coupling matrix elements, with Rydberg and continuum states of H<sub>2</sub> as the test cases. The principal contributions come from the excited electron's interactions with the oscillating finite monopole of the ion-molecule core. The electronic factors in the transition amplitudes are definitely dependent on internuclear distance, particularly in the cases of *p* and *d* states. The transition amplitudes accumulate their magnitudes over the full classically allowed range of internuclear distance, especially in the cases of *s* and *p* states. Specific application is made to vibronic coupling perturbations in *pσ* and *pπ* Rydberg states of H<sub>2</sub>.

### I. INTRODUCTION

The ground electronic states of molecules are, for the most part, well described by wave functions satisfying the Born-Oppenheimer approximation. It is becoming increasingly clear that the same does not hold true for molecular excited states. In small molecules, the coupling of nuclear kinetic and electronic energy is responsible, at least in part, for autoionization and predissociation. The same sort of coupling may give rise to associative ionization and associative detachment or to their inverses of dissociative recombination and dissociative attachment.

Penning ionization, electronic excitation transfer, and vibrational relaxation by electron-molecule collisions can also be induced by transfer of energy between nuclear kinetic and electronic degrees of freedom. Radiationless coupling among bound excited molecular states is associated with broad absorption bands, with anomalously long fluorescence

lifetimes, and with "missing" luminescence; the mechanism of this coupling is generally accepted to be due in major part to breakdown of the Born-Oppenheimer approximation.

It is our purpose here to develop a general theoretical and computational approach to handle a rather large class of phenomena, particularly for small molecules. These include autoionization, predissociation, associative ionization and dissociative recombination, excitation transfer, vibrational relaxation of molecule ions by collision with electrons, and the phenomenon developed most fully in this paper, the vibronic coupling of Rydberg states. We have given a preliminary account of our results for autoionization and predissociation.<sup>1</sup> These topics along with associative ionization and dissociative recombination, will be developed in subsequent work. Our approach, as we shall see, is restricted to relatively low energies, up to a few eV for the collision processes. In the present work, in the background<sup>2</sup> and preliminary application<sup>1</sup> present-

ed previously, and in the work immediately following this, we restrict our computations to excited bound and free states of  $H_2$ . This restriction permits us to make simplifications that would make our results less trustworthy for some more complicated molecules but that are entirely valid for  $H_2$ .

The class of problems of interest to us is, in the main, the set of phenomena involving weak coupling of bound or free excited molecular states with free states. It is both natural and important to include also bound-bound coupling. The study of bound-state perturbations is not central to our long-range intent. It provides useful examples and is absolutely necessary for cases involving higher-order coupling. Our emphasis throughout is primarily on the microscopic aspects of the coupling rather than on the phenomenology.

Coupling of states may be considered as either a mathematical artifact of an approximate representation for an energy eigenstate or a time-dependent phenomenon arising from the manner in which a system is prepared. Which description one chooses is a matter more of taste than of substance. The cogent point is that one begins with a representation that one presumes makes the Hamiltonian approximately diagonal, and then introduces the coupling by examining those parts of the Hamiltonian that are not diagonal in the initial representation. The general phenomenological treatment of this coupling is very naturally carried out by Feshbach's method of projection operators.<sup>3</sup>

Many operators in the Hamiltonian may be responsible for the coupling. The electron-electron repulsion operator couples bound atomic and molecular electronic functions to give configuration interaction (CI). Fano showed<sup>4</sup> how the concept of configuration interaction can be extended to the coupling of bound and free (ionic) states of atoms; Fano and Cooper<sup>5</sup> and Comes and Sälzer<sup>6</sup> carried out calculations describing coupling of quasibound autoionizing atomic states with the continuum in which these states are imbedded. Mies<sup>7</sup> has recently extended this work to the case of several closely spaced quasibound states interacting with and through a continuum.

In this paper, we describe the model, the general conclusions, and some specific inferences, particularly about bound-bound couplings, for *vibronic* coupling in  $H_2$ . Many of the inferences are as apt for heavier molecules as they are for  $H_2$ , and others deserve investigation to determine the extent of their applicability. In the following papers, we apply the method described here to the problems of autoionization and predissociation, and of associative ionization and dissociative recombination.

## II. MODEL

The setting up of the coupling problem falls naturally into two main parts, the choice of represen-

tation and the choice of coupling operator. The most attractive representation is one which corresponds closely to a realistic initial state of a time-dependent system, and is tractable for computation. We choose a Born-Oppenheimer basis set of zero-order functions and describe the coupling in terms of mixing among the Born-Oppenheimer states. Thus, if  $\Psi_\alpha$  is the total wave function for the state  $\alpha$  of the molecule of interest, we represent  $\Psi_\alpha$  as a product of an electronic function, a vibrational function  $\chi_{\alpha v}(\{\vec{R}\})$ , and a rotational function  $\Theta_{\alpha VK}(\omega)$ . For the situations we shall describe, we may represent the electronic wave function as a product of a function  $\Phi$  describing the core electrons and a one-electron function  $\psi_\alpha(\vec{r}, \{\vec{R}\})$  describing the active electron. Thus,

$$\Psi_\alpha(\{\vec{r}\}, \{\vec{R}\}) = \Phi_\alpha \psi_\alpha(\vec{r}, \{\vec{R}\}) \chi_{\alpha v}(\{\vec{R}\}) \Theta_{\alpha VK}(\omega). \quad (1)$$

We let  $\{\vec{r}\}$  and  $\{\vec{R}\}$  denote the totality of electronic and nuclear coordinates. The unindexed electron coordinates  $\vec{r}$  are those of the active electron. We simplify immediately to a diatomic so that  $\{\vec{R}\}$  can be replaced by the single variable  $R$ .

The coupling operator may be the electron correlation operator, the nuclear kinetic-energy operator, the spin-orbit coupling operator, or some combination of these. Others could also be used but may often be shown to be derivable from one of these three. For example, the dipole-dipole coupling operator used in the weak interaction coupling for excitation transfer and associative ionization model of Katsurra, Watanabe, and Mori<sup>8-11</sup> can be derived from the use of the nuclear kinetic-energy operator and Born-Oppenheimer basis functions. For present purposes, we restrict ourselves to the nuclear kinetic-energy operator  $\mathcal{T}_N$ . It is this restriction which permits us to write the electronic function in terms of the product of the core function  $\Phi$  (which does depend on  $R$ ) and the wave function  $\psi_\alpha(r, R)$  of the active electron. For the  $H_2$  problem, in the energy region of the ionization threshold, correlation coupling or bound-free configuration mixing is not important. In other molecular cases, e.g.,  $NO^{12}$ , it may be as important as coupling through nuclear kinetic energy or even may become the dominant mechanism.

## III. ELECTRONIC FUNCTIONS AND FACTORS

Whatever the coupling operator may be, if the wave functions are written in the form (1), we recognize immediately that a large variety of processes can all be viewed as special cases of the general phenomenon of diabatic coupling. Distinctions among the cases depend entirely on whether the initial (*i*) and final (*f*) states, electronic and vibrational, are bound or free. For example, if

$\psi_i$  and  $\chi_i$  are both bound and  $\psi_f$  is free while  $\psi_f$  is bound, the process corresponds to autoionization. If  $\psi_f$  is bound but  $\chi_f$  is free, the process is predissociation. Table I contains a classification of most of the processes that fall into the general category of diabatic coupling.

The method of obtaining Born-Oppenheimer wave functions was described, previously.<sup>2</sup> We use a model Hamiltonian based on the  $H_2^+$  wave function of Bates, Ledsham, and Stewart.<sup>13</sup> The effective potential, Coulomb and local approximation to exchange, is expanded in spherical harmonics. We have used only the monopole Coulomb and exchange and quadrupole Coulomb parts of the potential. Electronic wave functions and, for Rydberg states, energy eigenvalues were determined by numerical integration (Numerov procedure) for values of  $R$  from 1 to 5 a.u. Vibrational wave functions were also determined by Numerov's method. For  $H_2^+$ , the potential curve of Wind,<sup>14</sup> based on the calculations of Bates, Ledsham, and Stewart,<sup>13</sup> was used; this curve was also used to represent Rydberg states with  $n \geq 6$ . For lower Rydberg states, we used the potential curves corresponding to our computed electronic-energy eigenvalues. We also carried out some calculations, particularly for the case of associative ionization, with a potential curve given by Davidson<sup>15</sup> for the higher  $^1\Sigma$  state dissociating to  $H(n=1) + H(n=3)$ . This curve crosses the  $H_2^+$  curve at about  $R=1.5$  a.u. and, therefore, serves as a model for exploring the importance of curve-crossing. All integrations were outward only. For bound states, the smallness of the eigenfunction in the classically forbidden region at large  $R$  was the criterion for an approximation eigenvalue and eigenfunction. For continuum functions, the integrations were carried to sufficiently large  $R$  that the computed function fitted smoothly with the appropriate asymptotic form: spherical Bessel functions in the case of vibrational continuum functions, and Coulomb functions for electronic continuum func-

tions. Thus, the basis functions for the calculation are a self-consistent set of *adiabatic-state functions of the compound system*.

The choice of such a set is important for several reasons; some are fundamental to the physics and some are useful for facilitating the calculations. Let us first point out the most important reason for using adiabatic compound-state functions. We calculate initial and final electronic-state functions and initial and final vibrational-state functions all on the same basis, with the same total adiabatic Hamiltonian, whether the functions represent bound or free states.

A second reason for the choice of our Hamiltonian and compound system model is that the basis functions remain eigenfunctions of the Born-Oppenheimer Hamiltonian at all times and are, therefore, also orthogonal throughout a collision or decay process. The orthogonality and retention of the same Hamiltonian for all times conserve particles and eliminate any "post-prior" problems which occur in some treatments of rearrangement collisions. Furthermore, the property that the electronic wave functions are eigenfunctions of the Born-Oppenheimer Hamiltonian is useful for calculating the electronic factor of the most important type for our system:

$$F(nlm; k\lambda\mu; R) = \int \psi_{k\lambda\mu}^*(\vec{r}, R) \frac{\partial}{\partial R} \psi_{nlm}(\vec{r}, R) d\vec{r}. \quad (2)$$

Because the functions  $\psi_\alpha$  are eigenfunctions of the static electronic Hamiltonian

$$\mathcal{H}_0 = \mathcal{T}_{el} + \mathcal{V}(\vec{r}, R), \quad (3)$$

so that

$$\mathcal{H}_0 \psi_\alpha = \epsilon_\alpha \psi_\alpha, \quad (4)$$

TABLE I. Classification of molecular excited-state radiationless coupling processes. a, b

$\psi_i$	$\chi_i$	$\psi_f$	$\chi_f$	Type of process
<i>B</i>	<i>B</i>	<i>B</i>	<i>B</i>	Configuration mixing or vibronic coupling
<i>B</i>	<i>B</i>	<i>F</i>	<i>B</i>	Auto-ionization
<i>B</i>	<i>B</i>	<i>B</i>	<i>F</i>	Predissociation
<i>F</i>	<i>B</i>	<i>B</i>	<i>F</i>	Dissociative recombination
<i>B</i>	<i>F</i>	<i>F</i>	<i>B</i>	Associative ionization (inverse of dissociative recombination)
<i>B</i>	<i>F</i>	<i>F</i>	<i>F</i>	Penning ionization or collisional ionization
<i>B</i>	<i>F</i>	<i>B'</i>	<i>F'</i>	Electronic excitation transfer
<i>F</i>	<i>B</i>	<i>F'</i>	<i>B'</i>	Vibrational relaxation by electron collision
<i>F</i>	<i>B</i>	<i>F</i>	<i>F</i>	Dissociation by electronic collision

<sup>a</sup>Some three-body processes are omitted and, with one exception, inverse processes are also not specifically named.

<sup>b</sup>*B, B'* = bound; *F, F'* = free; *i* = initial, *f* = final;  $\psi$  = electronic function;  $\chi$  = vibrational function.

we may construct the commutator  $[\mathfrak{H}_0, \partial/\partial R]$  to derive the relation

$$F(nlm; k\lambda\mu; R) = (\epsilon_{nlm} - \epsilon_{k\lambda\mu})^{-1} \int \psi_{k\lambda\mu}^* \frac{\partial \psi_{nlm}}{\partial R} d\mathfrak{r}. \quad (5)$$

In general, (5) is considerably easier to compute than is (2), particularly when one or both  $\psi$  are a continuum function.

The total vibronic perturbation consists of the (negatives of the) two terms

$$T_1 = [\psi_f \chi_f | (\partial \psi_i / \partial R) (\partial \chi_i / \partial R)], \quad (6)$$

(in units of  $2\hbar^2/M_H$ ),

$$\text{and } T_2 = \frac{1}{2} (\psi_f \chi_f | (\partial^2 \psi_i / \partial R^2) \chi_i). \quad (7)$$

(We let  $M_H$  = mass of the hydrogen atom.) (The term in  $\partial^2 \chi / \partial R^2$  vanishes when  $i \neq f$  and, of course, is included in the diagonal terms.) For the  $H_2^+ + e$  case considered here, and for the  $p\sigma$  and  $p\pi$  states we have examined, the term in  $\partial^2 \psi_i / \partial R^2$  makes a contribution only a few percent of that of the term in  $(\partial \psi_i / \partial R) (\partial \chi_i / \partial R)$  and has, therefore, been neglected.<sup>16</sup> It must be included when computations reach the level of accuracy of optical spectroscopic measurements.

We have thus far considered no perturbations arising from the rotational part of the kinetic energy. These are known to exist and reflect themselves as  $l$ -uncoupling.<sup>17</sup> However, time-scale arguments given previously<sup>18</sup> imply that the vibrational perturbations are considerably more important than rotational perturbations for nuclear rotational quantum numbers  $K \lesssim 15$  or 20. The neglect of the rotational coupling terms keeps  $K$  as a constant of

the motion. Our calculations have been carried out for many different  $K$  states, particularly for the collisional problems for which contributions from relatively large impact parameters may be important.

The procedure in the calculations was generally as follows. For a given bound electronic state  $\alpha$ , the electronic energy  $\epsilon_\alpha(R)$  and electronic eigenfunction  $\psi_\alpha(\mathfrak{r}, R)$  were determined by numerical (Numerov) integration. Segmental linear fits were made to the functions:

$$E_\alpha(R) = \epsilon_\alpha(R) + E(H_2^+; R) + 0.55556 \text{ a.u.},$$

with values calculated at  $R = 1.0, 2.0, 3.0,$  and  $4.0$  a.u. The constant 0.55556 a.u. is the negative of the energy of  $H(n=1) + H(n=3)$ , relative to that of  $2H^+ + 2e$ , all far apart and with zero kinetic energy. From the effective potential

$$U(R) = E_\alpha(R) + \hbar^2 K(K+1)/M_H R^2,$$

the bound eigenvalues for vibration and the bound and free vibrational functions  $\chi_\alpha(R)$  were generated numerically. The electronic factors  $F[nlm; k(\text{or } n)\lambda\mu; R]$  were computed from Eq. (5) for several values of  $R$  and fit with a series of linear interpolations for intermediate values of  $R$ . Then the matrix elements  $T_1$  were evaluated, and from them the appropriate cross section or lifetime, depending on the case at hand.

The analytic expressions for the electronic energies  $E_\alpha(R)$  are as follows: (States are identified by the united atom notation for the orbital of the series electron. The second electron is always in the  $1s\sigma_g$  or  $\sigma_g 1s$  orbital, and no singlet-triplet splittings are taken into account. Energies are in atomic units of 27.210 eV.)

$$4s\sigma_g: E(R) = 0.0802 \{1 - \exp[-0.825(R - 2.038)]\}^2 + 0.0037 \exp[-4(R-4)^2] - 0.0802,$$

$$3d\sigma_g: E(R) = 0.1070 \{1 - \exp[-0.787(R - 1.998)]\}^2 + 0.0021 \exp[-4(R-4)^2] - 0.1070,$$

$$4d\sigma_g: E(R) = 0.0794 \{1 - \exp[-0.873(R - 1.992)]\}^2 + 0.0072 \exp[-4(R-4)^2] - 0.0794,$$

$$5p\sigma_u: E(R) = 0.0708 \{1 - \exp[-0.917(R - 1.995)]\}^2 + 0.0081 \exp[-4(R-4)^2] - 0.0708,$$

$$3p\pi_u: E(R) = 0.1111 \{1 - \exp[-0.753(R - 2.02)]\}^2 - 0.0012 \exp[-4(R-4)^2] - 0.1111,$$

$$4p\pi_u: E(R) = 0.0813 \{1 - \exp[-0.0857(R - 2.00)]\}^2 + 0.0062 \exp[-4(R-4)^2] - 0.0813,$$

$$4d\pi_g: E(R) = 0.0792 \{1 - \exp[-0.827(R - 2.045)]\}^2 + 0.0052 \exp[-4(R-4)^2] - 0.0792,$$

$$5d\pi_g: E(R) = 0.0680 \{1 - \exp[-0.921(R - 1.991)]\}^2 + 0.0080 \exp[-4(R-4)^2] - 0.0680,$$

$$3d\delta_g: E(R) = 0.1040 \{1 - \exp[-0.754(R - 2.048)]\}^2 - 0.0017 \exp[-4(R-4)^2] - 0.1040.$$

The electronic factors  $F(nlm; k\lambda\mu; R)$  of Eq. (5) depend very much on the internuclear distance  $R$ . However, they are almost independent of the principal quantum number  $n$  of the bound electronic state, for a given  $l$  (fixed for both initial and final states) and a given energy  $\frac{1}{2}k^2$  for the electron in its free state. Some examples of the functions  $F(R)$  are shown in Fig. 1. Clearly, evaluation of vibronic coupling requires the determination of the electronic functions over a wide range of  $R$ , particularly for the  $p$  and  $d$  states. Unfortunately, we cannot expect to get useful information about these processes by evaluating  $F(nlm; k\lambda\mu; R)$  at  $R=R_e$ , except when at least one of the states of interest is in a very low vibrational state.

The independence of the electronic factors  $F(nlm; k\lambda\mu; R)$  with respect to  $n$  is a reflection of the dependence of the amplitude of the inner part of the bound-state wave functions  $\psi_{nlm}$  and of the similarity of these functions for various values of  $n$  but the same values of  $l$  and  $m$ .

#### IV. NUCLEAR INTEGRATIONS AND CLASSIFICATION OF DIABATIC TRANSITIONS

One diagnostic study was particularly enlightening with regard to the role of curve crossings and the portion of the range of  $R$  over which transition amplitude is accumulated. We examined several typical cases corresponding to associative ionization processes by performing a partial integration of the matrix element from the origin to successively larger values of the outer limit  $R$ . This function

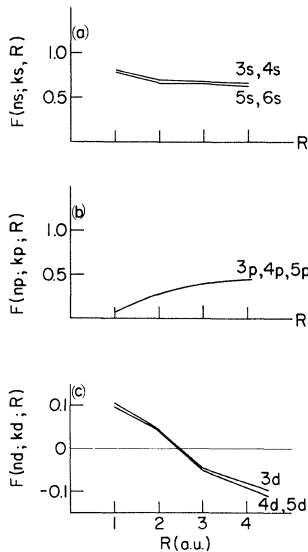


FIG. 1. Electronic factor  $F(nlm; k\lambda\mu; R)$  of the transition amplitude, as a function of the internuclear distance  $R$  [see Eq. (5) of text].

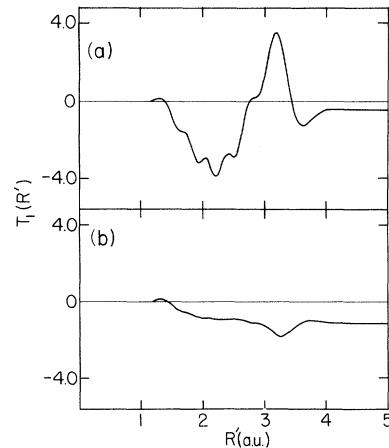


FIG. 2. Transition amplitude integrals  $T_1(R')$  for associative ionization and dissociative recombination, as functions of the upper limit  $R'$  of integration. Note that the functions  $T_1(R')$  for the  $p$  state, in (a), do not settle down to their final value until  $R' \sim 4$  a.u.: (a) bound Rydberg orbital,  $5p\sigma$ ; nuclear kinetic energy in the dissociated state,  $10^{-3}$  a.u.; vibrational state of  $H_2^+$ ,  $v=4$ ; rotational state,  $K=4$ ; and (b) bound Rydberg orbital,  $5d\pi$ ; nuclear kinetic energy in the dissociated state,  $10^{-3}$  a.u.; vibrational state of  $H_2^+$ ,  $v=4$ ; rotational state,  $K=4$ .

$$T_1(R') = \int_0^{R'} \chi_f(R) F(f; i; R) \left( \frac{\partial \chi_i}{\partial R} \right) dR$$

$$\rightarrow T_1 \text{ as } R' \rightarrow \infty$$

shows quite explicitly where the transition amplitude arises. Admittedly, this kind of diagnosis depends on what form one uses for integration. Suppose we were able to transform the  $R$  derivative into an operator proportional to  $\partial E_\alpha(R)/\partial R$  as we did with  $\partial\psi/\partial R$  or as one does in making the transformation of optical transition amplitudes from dipole velocity to dipole length. Then we would find an  $R$  dependence of  $T_1(R')$  differing from that of the form just given. This is quite analogous to the different distance dependences of the dipole-length, velocity, and acceleration expressions for optical transitions. Despite such ambiguities, if we calculate  $T_1(R')$  in the same way for several types of transitions, we can make a useful comparison among them.

Figures 2(a) and 2(b) show two straightforward examples, the transition amplitude for  $H(n=1) + H^*(n=3)$  colliding to give  $H_2^+ + e$ . These curves are taken for initial relative kinetic energy of  $H$  and  $H^*$  of  $10^{-3}$  a.u., for final vibrational and rotational quantum numbers  $v=4$  and  $K=4$ . Figure 2(a) corresponds to the  $5p\sigma_u$  state, and Fig. 2(b) to the  $5d\pi_g$  state, in the united atom notation. Clearly, the  $5p\sigma_u$  example shows accumulation of probability amplitude everywhere between circa  $R=1.2$  and

$R=4$  a.u. The  $5d\pi$  example is governed in a large part by the behavior near the left-hand turning point when  $1.2 \lesssim R \lesssim 2$  a.u. This is due in part to the zero in the electronic factor  $F(f; i; R)$  near  $R=2.5$  a.u.

A more complicated example, but equally enlightening, is the state whose united atom description is the  $4s\sigma_g$  for small values of  $R$ . The  $4s\sigma_g$  and  $4d\sigma_g$  curves show an avoided crossing between  $R=2$  and  $R=3$  a.u. The energies of these states are discussed in Sec. VI. The lower energy of the two is  $4s$ -like for  $R \leq 2$  and  $4d$ -like for  $R \geq 3$ . The accumulation of transition amplitude for the process  $H+H^* \rightarrow H_2^+ + e$  in this case is of some interest. For small values of  $R$ , the principal contribution to the outgoing electron wave is the  $s$  wave, and, as Fig. 3(a) shows, this amplitude accumulates over much of the range of  $R$  from 1.2 to 2.7 a.u. Over this same range, a small negative  $d$ -wave amplitude is developed, originating largely near the left turning point, at about 1.5 a.u. When the state changes character from  $s$  to  $d$ , a sharp oscillation develops in the  $d$ -wave amplitude; this is most clearly demonstrated by the sharp peak at about 3.3 a.u. in the  $d$ -wave amplitude, as shown in Fig. 3(b). The net result of the oscillation leaves the total  $d$ -wave amplitude relatively small and positive. The outgoing  $s$  wave is the larger by far and develops at relatively small internuclear distances, while the smaller  $d$ -wave contribution develops primarily

in the region of the pseudocrossing and secondarily near the left turning point. This kind of behavior can be expected to show itself in such phenomena as the dependence on vibrational quantum number of the angular distribution of photoelectrons or, more probably, of electrons from autoionization of Rydberg states. Calculations of the type used to generate Fig. 3 were also carried out with a potential curve that crosses the  $H_2^+$  curve.<sup>15</sup> When such a curve is used, the results are virtually identical to those in Fig. 3. In other words, the proximity of the curves of  $H+H^*$  and  $H+H^+$  and the relatively small change in nuclear momentum associated with the transition make the entire range of  $R$  important for this transition. In this example, the effects of a crossing point are entirely negligible.

This conclusion has led us to suggest that *predissociation* may occur from high vibrational states of one Rydberg state into the vibrational continuum of a lower Rydberg state.<sup>1</sup> The potential curves of the two states may be virtually identical, except for a vertical displacement. Such a predissociation process does not, at first sight, fit into any of the Franck-Condon cases of type 1 (electronic) predissociation classified by Herzberg.<sup>19</sup> However, we must look at this judgment in light of our conclusion about the unimportance of classical crossing points for transitions between similar and relatively close potential curves.

It becomes useful to classify curve crossing or diabatic transitions in a manner that differs a little from Herzberg's classifications of predissociation. Our classification is a generalization insofar as it encompasses all the processes in Table I; it is also a modernization insofar as it reflects our growing ability to make semiquantitative theoretical analyses of diabatic transitions, as well as inferential analyses from spectral data. We define three categories of diabatic molecular transitions, according to the range of  $R$  over which transition amplitude is principally accumulated: (i) the classic "crossing-point" case in which the dissimilarity of the two states makes the transition amplitude oscillate rapidly and average quickly to zero, except in the region of a crossing point [Fig. 4(a)]; (ii) the "turning-point" case in which the curves never cross but transitions do occur between them, with amplitude gathered primarily near the classical turning point for the initial and final states. These turning points must lie at values of  $R$  close together with respect to the widths of the turning-point lobes of the wave functions of initial and final states. Note that we must deal explicitly with separate effective potentials, including the centrifugal potential, for each rotational state of the molecule, in using the turning-point model. This case may be important for some cases of associative and Penning ionization, e.g., in  $He^*(2^3S, 2^1S) + Ar$  or  $Hg$  [Fig. 4(b)];

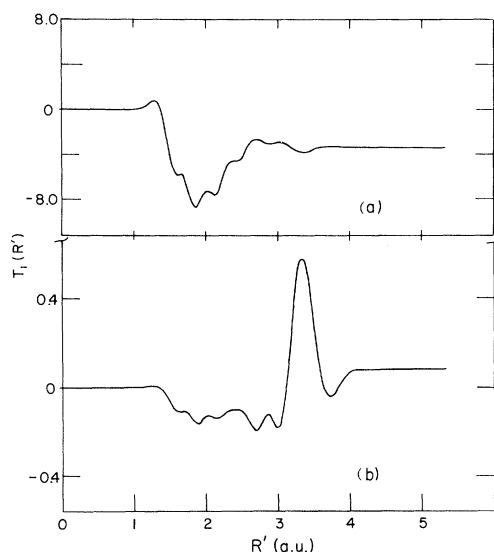


FIG. 3. Transition amplitude integrals  $T_1(R')$  for associative ionization and dissociative recombination as functions of  $R'$ , the upper limit of integration, for that  $\sigma_g$  bound state that is  $4s$ -like for small  $R$ : (a)  $s$ -wave component; nuclear kinetic energy of dissociated state,  $10^{-3}$  a.u.; vibrational state of  $H_2^+$ ,  $v=4$ ; rotational state,  $K=4$ ; (b)  $d$ -wave component, for the same states.

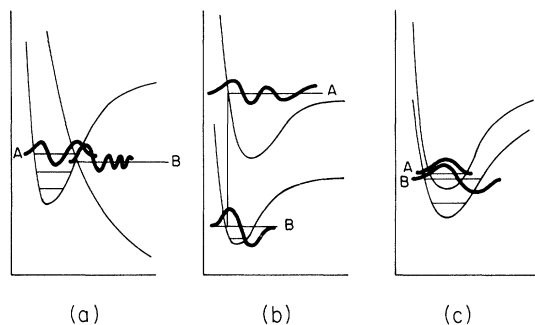


FIG. 4. Three cases of dependence of transition probability on internuclear distance: (a) Probability  $\neq 0$  only near crossing point; (b) probability  $\neq 0$  only near classical turning point, and no crossing or near-crossing occurs; (c) probability  $\neq 0$  over a wide range of internuclear distance. Transitions in all three cases are between states A and B.

(iii) the "broad-range" case in which transition amplitude accumulates or oscillates over much of the range of the potential well, as in the associative ionization of  $H_2$  [Figs. 2, 3, and 4(c)]. This third category appears to require the fullest treatment for its quantitative development. The first two cases lend themselves to distinct simplifications and, in some cases, to quite elegant treatment.<sup>20-23</sup> There will be other cases, such as that of transitions between curves that are close in a narrow range of  $R$  but never cross; such cases are trivial deviations from the three main categories and can be considered with them. There are also going to be cases that are clearly intermediate situations; these may require the full and perhaps heavy-handed treatment of category (iii). The classification also applies to large molecules with multidimensional potential surfaces, but we are only beginning to understand the role of Franck-Condon factors in diabatic transitions in these molecules.<sup>24, 25</sup>

It is clear from Fig. 3 that the autoionizing transitions and some associative-ionizing transitions we are examining for  $H_2$  fit category (iii) and Fig. 4(c). There is no reason to believe that this category is any more general than the other two. Transitions in category (iii) presumably tend to satisfy the vibrational propensity rule<sup>18</sup>

$$\text{prob}(\Delta v = \pm 1) \gg \text{prob}(\Delta v = \pm 2) \gg \dots$$

For autoionization of  $H_2$ , this seems to be the case, but for auto-ionization of  $N_2$  it appears otherwise, according to recent work of Berkowitz and Chupka.<sup>26</sup> Sometimes we can expect only one category of transition to be available. However, when more than one category is open, we do not have any ready way, as yet, to decide which will

be the more available, short of doing rather full calculations.

An interesting phenomenon in associative ionization arises from certain low-energy collisions. This is the appearance of a sharp maximum in one set of the transition probabilities for associative ionization, from the (united atom)  $4s\sigma$ ,  $K=6$ , channel into various vibrational states of  $H_2^+$ . It occurs when the kinetic energy of relative motion of H and  $H^*$  is  $1.2 \times 10^{-4}$  a.u. ( $\frac{1}{25}$  of normal thermal energy). From an integral development like those of Figs. 2 and 3, the peak appears to be a straightforward result of a fortuitously good match of the free vibrational function and the distance derivative of the bound vibrational function, especially between 1.5 and 1.7 a.u., and again between 1.8 and 2.0 a.u. Examples of the nuclear wave functions are shown in Fig. 5. The cross sections for three vibrational states of  $H_2^+$  are shown as functions of energy in Fig. 6; clearly the vibrational state influences only the magnitude of these resonancelike curves. Note that although the peaks of the curves are high, their contributions to ordinary experimental-rate constants are small because the corresponding low-energy collisions are rare.

#### V. VIBRONIC INTERACTIONS AMONG RYDBERG STATES

We have investigated the vibronic coupling of Rydberg states by way of a model, albeit a rather

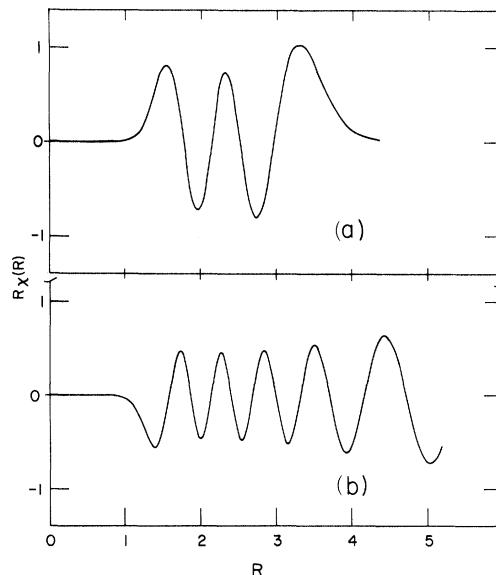


FIG. 5. Nuclear wave functions for states showing resonancelike peak in associative ionization cross sections: (a) Bound function for  $H_2^+$ ,  $v=4$ ,  $K=6$ ; (b) free function for the  $4s\sigma$  state, with  $K=5$  and kinetic energy of  $1.2 \times 10^{-4}$  a.u., corresponding to the maximum transition probability.

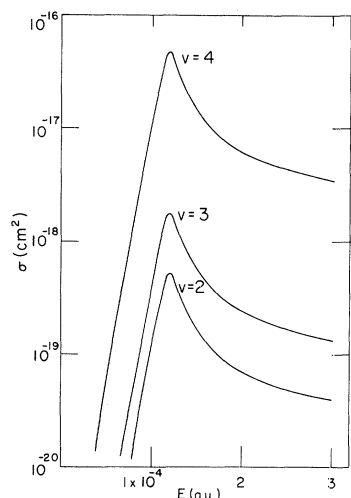


FIG. 6. Sharp maxima in squares of transition matrix elements for associative ionization in very low-energy collisions.

accurate one. We made our choice on the grounds that an attempt to reproduce actual spectroscopic perturbations would only be useful if its accuracy were comparable to that of spectroscopic measurements, and such accuracy is not yet attainable. The theoretically derived effects of vibronic coupling, like those of any interaction among bound states, depend on the ratios of the coupling matrix elements to the difference between unperturbed energy levels. Because the vibronic matrix elements are small, coupling is important only when unperturbed states are very close in energy, so that specific coupling depends in a very sensitive way on the energy levels of the unperturbed vibrational eigenstates. One might try to devise a semiempirical scheme for obtaining these eigenstates by deperturbing experimental spectra, or one might do as we have, use a single self-consistent model to test the grosser features of vibronic coupling. We have used the same potential curve for all Rydberg states of the same  $l$  and  $\lambda$ , simply displaced vertically to correspond to the term values of the various  $n$  values. We have treated only the  $np\sigma$  and  $np\pi$  states, which can be reached optically from the ground state. We have limited ourselves to the case  $K=0$ . From this treatment, we have determined the region of quantum numbers in which one can expect vibronic coupling to be important, and the magnitude of the number of states we may expect to be coupled together. We should not expect that any particular pair of states that happened to be coupled in the model will in fact be coupled in the real molecule.

The off-diagonal matrix elements of vibronic coupling fall, for the most part, in the range  $10^{-5} - 5 \times 10^{-4}$  a.u., or between 2 and  $100 \text{ cm}^{-1}$  for principal quantum numbers between 4 and 10. For

higher principal quantum numbers, the off-diagonal elements grow smaller, according to the scaling law  $(n_i n_f)^{-3/2}$ , analogous to that for autoionization.<sup>27</sup> To display how vibronic coupling affects Rydberg states of  $\text{H}_2$ , we show some selected portions of the energy matrices for  $np\sigma$  and  $np\pi$  states in Table II, and in Fig. 7 a schematic map indicating those states that are coupled relatively strongly. The criterion for grouping states together in this figure is that, for at least one pair in the group, the ratio

$$\left| \frac{\langle i | \mathcal{H} | j \rangle}{\langle i | \mathcal{H} | i \rangle - \langle j | \mathcal{H} | j \rangle} \right| > \frac{1}{5} .$$

States of low  $n$  and  $v$  are not coupled because their energy separations are too large. Note that for lower values of  $n$ , states of consecutive  $n$  values tend to couple, but for higher values of  $n$ , coupling is primarily between states of rather different  $n$ . This is due to the fact that for sufficiently high  $n$ , the vibrational spacing is larger than the difference in electronic term values.

The level shifts are given for the vibronically interacting states shown in Table II. Even before

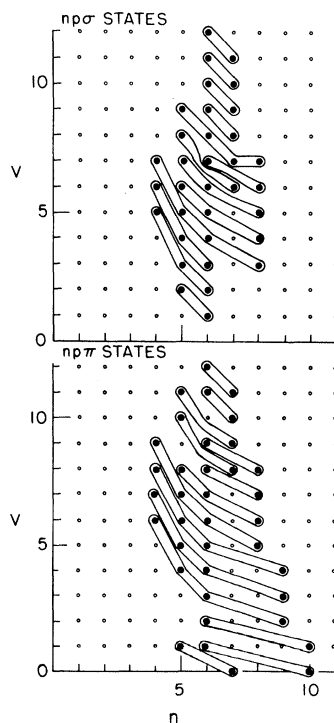


FIG. 7. Schematic representation of the groups of levels *strongly* coupled by vibronic interactions. Principal quantum numbers  $n$  increase along the abscissa; vibrational quantum numbers  $v$  increase along the ordinate. Closely coupled sets of states are shown inside the closed loops.

TABLE II. Selected parts of the vibronic interaction matrix for strongly coupled Rydberg states. (Matrix elements are in units of  $10^{-3}$  a.u.) The energy scale of each matrix has been shifted by adding a unit matrix multiplied by the constant shown in the upper left corner of each matrix; the shift was made to make it as convenient as possible to recognize the diagonal differences. "Shifts" are the spectroscopic level displacements (in  $\text{cm}^{-1}$ ), of the  $n, v$  states in the order given in the matrices, relative to the corresponding unperturbed levels.

A. $np\sigma$ states													
594.05	$n$	$v$	$n$	4	5	6	569.61	$n$	$v$	$n$	5	6	8
			$v$	5	3	2				$v$	6	5	4
	4	5		2.23	0.07	0.00		5	6		0	0.40	0.03
	3				2.12	0.30		6	5			0.47	0.19
	2					0		8	4				0.03
	Shifts: +9.4, -0.4, -9.1 $\text{cm}^{-1}$ .												
577.88	$n$	$v$	$n$	4	5	6	562.87	$n$	$v$	$n$	5	6	8
			$v$	7	5	4				$v$	7	6	5
	4	5		0.05	0.11	0.02		5	7		0	0.42	0.03
	3				1.02	0.37		6	6			0.98	0.02
						0.97		8	5				1.06
	Shifts: -2.7, -46.2, +94.4, -45.4 $\text{cm}^{-1}$ .												
585.21	$n$	$v$	$n$	4	5	6	544.42	$n$	$v$	$n$	6	7	8
			$v$	6	4	3				$v$	9	8	
	4	5		0.64	0.08	0.01		6	9		1.22	0.47	
	3				0.58	0.34		7	8			0	
	Shifts: +30.6, +3.9, -34.6 $\text{cm}^{-1}$ .												
538.72	$n$	$v$	$n$	6	7	9	533.29	$n$	$v$	$n$	6	7	10
			$v$	10	9	0				$v$	11	10	7
	6	7		0.71	0.49	0		6	11		0	0.51	0.30
	9							7	10				
	Shifts: +55.0 $\text{cm}^{-1}$ .												
	Shifts: +83.7 $\text{cm}^{-1}$ .												



trying to interpret specific shifts in the spectrum of  $H_2$ , we can expect such shifts to appear and to be large enough to cause some difficulties in assignments. It may be possible in time to infer experimental values of the coupling terms by deperturbing experimental spectra taken under sufficiently high resolution.<sup>28</sup>

### VI. CORRECTION

In the course of this work, we discovered an error in our earlier computation<sup>2</sup> of the zero-order adiabatic  $s$  states in the potential of  $H_2^+$ . We have recalculated the Rydberg-term values for the  $ns$  and  $nd$  states ( $n=3-6$ ) in the spherically symmetric potential  $V_{0CE}$  and then diagonalized the matrices of the  $m_l=0$  ( $s$  and  $d$  states) in the monopole-plus quadrupole potential  $V_{0CE} + V_{2C}$ . These results, corrections to Table I and Table II of Ref. 2, are given here in Table III. We also include the  $3d\sigma$  and  $4d\sigma$  states in order to show how the avoided crossing of  $3s$  and  $3d\sigma$ , and of  $4s$  and

$4d\sigma$ , is introduced by the  $l$ -spoiling potential  $V_2$ .

The previous results placed the  $ns$  levels below the corresponding  $nd$   $s$  at all internuclear distances. This is physically incorrect, as Mulliken has emphasized.<sup>29</sup> We had originally attributed this to an artifact of the model; fortunately it is not, and was due only to a program error. The corrected level diagram is now consistent with the known level shown for  $H_2$ .

We have already referred to the curve-crossing behavior in the  $4s\sigma$  and  $4d\sigma$  states. A similar effect occurs with the other curves ( $n=3, 5$ , and  $6$ ) between  $R=1$  and  $R=2$  a. u. The mixing and avoided crossings induced in these states by the nonspherical potential are the most dramatic example of  $l$  spoiling in the model. This behavior naturally gives rise to large contributions to vibrationally induced transition amplitudes because of the large values of  $\partial\psi/\partial R$  in the crossing regions.

The worst  $l$  spoiling in the  $\sigma_g$  states occurs in the neighborhood of the equilibrium separation because of the avoided crossing in the adiabatic

TABLE III. Corrected eigenvalues for the adiabatic states. (Energy in Hartree a.u. 27.21 eV; distances in Bohr radii).

A. Rydberg states in the potential $V_{0CE}$					
$ns$	$R=$	1.0	2.0	3.0	4.0
3		-0.0697	-0.0603	-0.0532	-0.0472
4		-0.0368	-0.0331	-0.0302	-0.0276
5		-0.0227	-0.0209	-0.0194	-0.0181
6		-0.0154	-0.0144	-0.0135	-0.0128
$nd$					
3		-0.0578	-0.0587	-0.0584	-0.0583
4		-0.0324	-0.0328	-0.0328	-0.0324
5		-0.0206	-0.0208	-0.0208	-0.0206
6		-0.0143	-0.0143	-0.0143	-0.0142
B. Rydberg gerade states with $m_l=0$ , in the potential $V_{0CE} + V_{2C}$ . <sup>a</sup>					
$nl$					
6s		-0.0154	-0.0144	-0.0135	-0.0128
6d		-0.0144	-0.0145	-0.0146	-0.0146
5s		-0.0227	-0.0208	-0.0194	-0.0181
5d		-0.0207	-0.0212	-0.0214	-0.0215
4s		-0.0368	-0.0332	-0.0301	-0.0275
4d		-0.0326	-0.0324	-0.0341	-0.0344
3s		-0.0697	-0.0600	-0.0531	-0.0471
3d		-0.0582	-0.0609	-0.0628	-0.0648

<sup>a</sup>States are listed according to whether the  $l=0$  or  $l=2$  component dominates. For  $n=3$  and  $n=6$ , the ratios of dominant component to the other component are circa 2.2:1 and 3:1, respectively, so that these are actually mixtures of  $s$  and  $d$  states.

limit. This is a reflection of the transition that occurs around  $R \approx 2$  from the separated-atom to the united-atom situation. Over most of the range  $1 \leq R \leq 4$  a.u., for the  $4s$  and  $4d$  states, about 10% of the minor component appears in the other; for  $5s$  and  $5d$ , about 12%; and for  $6s$  and  $6d$ , for which the zero-order states are almost degenerate, 25% of each component mixes with the other. For large  $R$ , e.g.,  $R = 4$  a.u., the mixing is much less than for  $R = 2$ , and consists of about equal amounts mixing of states  $n'l$  and of states  $n$  with a given  $nl'$  state. Note that one must be cautious not to

make very specific inferences about  $l$  spoiling in real rotation-vibration states of  $H_2$  on the basis of the model, insofar as the occurrence of near degeneracies and therefore the specific values for shifts and mixing coefficients are very model-sensitive. The model is useful to tell us about how large the maximum  $l$  spoiling will be, and to give us a rough idea at about what  $R$  value this can be expected, but one must not trust the present model for quantitative reproduction of the detailed properties of  $H_2$ .

<sup>1</sup>S. E. Nielsen and R. S. Berry, Chem. Phys. Letters 2, 503 (1968).

<sup>2</sup>R. S. Berry and S. E. Nielsen, J. Chem. Phys. 49, 116 (1968).

<sup>3</sup>H. Feshbach, Ann. Phys. (N. Y.) 19, 287 (1962).

<sup>4</sup>U. Fano, Phys. Rev. 124, 1866 (1961).

<sup>5</sup>U. Fano and J. W. Cooper, Phys. Rev. 138, A1364 (1965).

<sup>6</sup>F. J. Comes and H. G. Sälzer, Phys. Rev. 152, 24 (1966).

<sup>7</sup>F. H. Mies, Phys. Rev. 175, 164 (1968).

<sup>8</sup>M. Mori, T. Watanabe, and K. Katsuura, J. Phys. Soc. Japan 19, 380 (1964).

<sup>9</sup>K. Katsuura, J. Chem. Phys. 42, 3771 (1965).

<sup>10</sup>T. Watanabe, J. Chem. Phys. 46, 3741 (1967).

<sup>11</sup>T. Watanabe and K. Katsuura, J. Chem. Phys. 47, 800 (1967).

<sup>12</sup>J. N. Bardsley, J. Phys. B1, 349, (1968); B1, 365 (1968).

<sup>13</sup>D. R. Bates, K. Ledsham, and A. L. Stewart, Phil. Trans. Roy. Soc. London A246, 215 (1953).

<sup>14</sup>H. Wind, J. Chem. Phys. 42, 2371 (1965); 43, 2956 (1965).

<sup>15</sup>E. R. Davidson, thesis, Indiana University, 1961, AFOSR Contract No. 49 (638)-318 (unpublished); J. Chem. Phys. 35, 1189 (1961).

<sup>16</sup>F. Bloch and N. E. Bradbury, Phys. Rev. 48, 689 (1935), show that the ratio  $T_1/T_2$  is often about the ratio of the vibration amplitude to the equilibrium internuclear

distance. However, for the  $\sigma_g$  states of  $H_2$ , the  $T_2$  is quite important, as Secs. IV and VI of the present work indicate.

<sup>17</sup>M. Ginter, J. Chem. Phys. 46, 3687 (1967) and Refs. therein.

<sup>18</sup>R. S. Berry, J. Chem. Phys. 45, 1228 (1966).

<sup>19</sup>G. Herzberg, Spectra of Diatomic Molecules (D. Van Nostrand Co., Inc., Princeton, N. J., 1955), pp. 413-414 and 420-432.

<sup>20</sup>E. E. Nikitin, J. Chem. Phys. 43, 744 (1965).

<sup>21</sup>E. E. Nikitin, Opt. i Spektroskopiya 22, 689 (1967) [English transl. Opt. Spectry. (USSR) 22, 379 (1967)].

<sup>22</sup>E. I. Dashevskaya and E. E. Nikitin, Opt. i Spektroskopiya 22, 866 (1967) [English transl.: Opt. Spectry. (USSR) 22, 473 (1967)].

<sup>24</sup>W. Siebrand, J. Chem. Phys. 46, 440 (1967); 47, 2411 (1967).

<sup>25</sup>W. Siebrand and D. F. Williams, J. Chem. Phys. 49, 1860 (1968).

<sup>26</sup>J. Berkowitz and W. A. Chupka (to be published).

<sup>27</sup>J. N. Bardsley, Chem. Phys. Letters 1, 229 (1967).

<sup>28</sup>It has come to our attention that G. Herzberg and J. Shoosmith and also Y. Tanaka and T. Takamine are now analyzing the Rydberg spectrum of  $H_2$  in sufficient detail that the deperturbation may be feasible.

<sup>29</sup>R. S. Mulliken, J. Am. Chem. Soc. 86, 3183 (1964); 88, 1849 (1966); also R. S. Berry and S. E. Nielsen, the Rydberg states of molecules, part VII (to be published).